

# Honeycomb-Type Microscale Arrays for High-Pressure Hydrogen Storage

Mingming Wang<sup>1</sup>, Biao Xu<sup>1</sup>, Zesen Ren<sup>2</sup>, Hao Wu<sup>2</sup>, Renjing Cao<sup>2,\*</sup>

<sup>1</sup>Shenzhen Radiant Architectural Technology Co., Ltd., Shenzhen, China

<sup>2</sup>Department of Mechanics and Aerospace Engineering, Southern University of Science and Technology, Shenzhen, China

## Email address:

903654085@qq.com (Mingming Wang), winstonradiant@gmail.com (Biao Xu), 12132413@mail.sustech.edu.cn (Zesen Ren), wyh@mail.sustech.edu.cn (Hao Wu), caorj@sustech.edu.cn (Renjing Cao)

\*Corresponding author

## To cite this article:

Mingming Wang, Biao Xu, Zesen Ren, Hao Wu, Renjing Cao. Honeycomb-Type Microscale Arrays for High-Pressure Hydrogen Storage. *International Journal of Energy and Power Engineering*. Vol. 11, No. 6, 2022, pp. 125-131. doi: 10.11648/j.ijepe.20221106.12

**Received:** November 3, 2022; **Accepted:** November 18, 2022; **Published:** November 29, 2022

**Abstract:** Hydrogen is an important secondary renewable energy source, and its efficient use depends on the development of safe, economical, and portable hydrogen storage technology. Current hydrogen storage methods are divided into physical and chemical methods, and physical methods include three categories: low-temperature liquid storage, adsorption storage, and high-pressure gaseous storage. However, hydrogen can easily escape and undergo chemical reactions, being difficult to simultaneously meet requirements of safety, economy, and portability. A honeycomb-structured tube bundle made of glass fiber for high-pressure gaseous hydrogen storage has been proposed to overcome shortcomings of existing methods both theoretically and experimentally. To further develop this technology, various structural adjustments and improvements are introduced. Microscale cylindrical tubes made from glass fibers produced using optical fiber technology are combined in an array (bundle), and the array surface is protected by a steel sleeve. The array is completely closed at one end, and high-pressure hydrogen (100 MPa) can be rushed into the other end for storage or transportation. Unlike the existing thin-walled tube bundle and external hexagonal honeycomb structure, thick-walled tube bundles are directly used to form a honeycomb structure, and different protective sleeve materials are tested. The influence of various parameters, such as number of tubes and wall thickness, on the hydrogen storage performance of the tube bundle is evaluated using the finite element method. Comparing numerical and experimental results show that the number of tubes in a bundle is negatively related to the storage performance, and increasing the tube wall thickness increases performance up to a certain value, after which further thickening reduces performance.

**Keywords:** High-Pressure Hydrogen Storage, Honeycomb-Type Arrays, Glass Fiber, Microscale Structure

---

## 1. Introduction

With the ever-increasing energy demands, the huge potential of hydrogen energy should be properly exploited. Hydrogen is a well-known high-quality renewable energy resource owing to its simple production, economical batch acquisition, and null carbon emissions. In addition, hydrogen can be mixed with a variety of energy sources, being promising for energy storage and security [1]. However, hydrogen storage still faces several challenges. For instance, hydrogen can easily penetrate metals and cause embrittlement [2], greatly reducing yield stress and even leading to cracking. Therefore, storage materials must be

carefully selected. In addition, hydrogen can easily escape to the environment, especially from conventional canned storage. Hydrogen can even pass through a very small safety gap and become hazardous owing to its high activity. Thus, some deficiencies persist in hydrogen storage tanks. Moreover, given the costly conversion of gaseous hydrogen into liquid at low temperatures, its energy is slightly insufficient compared with that of solid energy at the same volume. Overall, the safety, economy, efficiency, and portability of hydrogen storage are remaining challenges that restrict its development [3].

Available hydrogen storage technologies are divided into physical and chemical methods. Physical methods include high-pressure gaseous hydrogen storage, low-temperature

liquid hydrogen storage, and low-temperature adsorption hydrogen storage [4]. The low-temperature storage method converts hydrogen into liquid and stores it in an insulated vacuum container. This storage method provides high storage density but requires high energy and cannot be used for long-term storage. Consequently, it is unsuitable for civil and commercial applications. Low-temperature adsorption storage uses the van der Waals interactions between porous materials and gas molecules for hydrogen storage. This method involves physical adsorption because the gas in molecular form does not dissociate. Nevertheless, given the weak van der Waals forces between porous materials and various gas molecules [5], suitable adsorption is only achieved at low temperatures ( $\sim 77$  K). High-pressure gaseous storage increases the density of stored gas by increasing the pressure at a certain temperature, and it is the most widely used storage method. This method is simple, provides fast gas filling and discharging, operates at normal temperatures, and has a low cost. However, current high-pressure gaseous hydrogen storage devices use metal cans, which may cause safety and operation problems.

Considering the honeycomb-structured hydrogen storage tube bundle introduced by Zhevago et al. [6], various adjustments for improved hydrogen storage are proposed herein. First, glass fiber tubes with a relatively large initial diameter are drawn from the preform and then spun into thick-walled cylindrical tube bundles with micron diameter. The tubes can also be spun into a flexible glass fiber bundle using optical fiber technology. The hexagonal shell is omitted, and many cylindrical tube bundles are directly arranged and sintered into an array. A protective sleeve wraps the bundle periphery. One end of the array is completely closed and the other end is connected to an adapter. When high-pressure hydrogen (100 MPa) is flushed, a tube bundle array with an enlarged length or diameter can be externally connected to reduce pressure to a usable range. Compared with conventional hydrogen storage tanks, this structure has the following advantages [7]:

- 1) Glass fiber is used for hydrogen storage, thus avoiding the embrittlement of metals caused by hydrogen and promoting long-term storage.
- 2) Glass fiber has a high tensile strength to improve robustness to hydrogen storage pressure and increase the efficiency of hydrogen energy in the same space.
- 3) A tight enclosure is achieved owing to the microscale tube bundle that mitigates the escape of hydrogen.
- 4) Safety is improved because even if a tube bundle breaks, massive gas leakage does not occur.
- 5) Portability is high, and the tube bundle array can be adjusted according to the transportation and use environment, thereby saving space. For example, in vehicle-mounted hydrogen storage, it can be laid along the vehicle frame without occupying other spaces to satisfy design and usability requirements.

The use of the finite element method in Ansys Workbench simulations conducted to investigate the influence of various parameters of the glass fiber tube bundles on hydrogen

storage is reported. The corresponding stress, weight capacity, and volume capacity are obtained. Comparisons with experimental results from other studies validate the simulation results of this study.

## 2. Design of Honeycomb-Type Arrays

### 2.1. Selection of Materials

Glass has many advantages as a hydrogen storage material. For instance, unlike metals, glass is not embrittled by hydrogen and has a lower thermal conductivity, which reduces the likelihood of hydrogen being pressurized by heating. On the other hand, the theoretical tensile strength of glass is high, but the actual strength of ordinary glass is only 60–80 MPa. Although the addition of  $B_2O_3$  or CaO can increase the tensile strength [8], it cannot reach an adequate value. The actual tensile strength is lower than the theoretical one because of inevitable defects in glass, such as cracks and bubbles. Such defects cause stress concentration. When the local stress exceeds the tensile strength, the glass breaks. The theoretical tensile strength,  $\sigma_t$ , can be expressed as

$$\sigma_t = \sqrt{\gamma \frac{E}{\alpha}} \quad (1)$$

where  $\gamma$  is the surface energy,  $E$  is the elastic modulus, and  $\alpha$  is the distance between atoms. For  $\gamma = 3.5 \text{ J/m}^2$ ,  $E = 60 \text{ GPa}$ , and  $\alpha = 0.2 \text{ nm}$ ,  $\sigma_t = 32 \text{ GPa}$ . Hence, glass can be used as a hydrogen storage material if its defects are minimized. By using optical fiber technology to spin glass into microscale glass fibers, its tensile strength can reach 2000 MPa. Based on the experimental results reported by Wen F. [9], the specifications listed in Table 1 are considered for finite element calculations using glass as the tube material.

**Table 1.** Mechanical parameters of glass fiber.

| Parameter                  | Value      |
|----------------------------|------------|
| Material                   | Fiberglass |
| $\rho$ , kg/m <sup>3</sup> | 2460       |
| $E$ , MPa                  | 80,000     |
| $\nu$                      | 0.22       |
| $\sigma_t$ , MPa           | 20,000     |
| $\sigma_c$ , MPa           | 500        |
| $\sigma_s$ , MPa           | 300        |

$\rho$ , density;  $E$ , Young modulus;  $\nu$ , Poisson ratio;  $\sigma_t$ , maximum tensile strength;  $\sigma_c$ , maximum compressive strength;  $\sigma_s$ , maximum shear strength.

### 2.2. Honeycomb-Type Arrays

Using optical fiber technology, glass is spun into microscale cylinders, and several identical cylinders are arranged. A protective sleeve is wrapped around the surface of the honeycomb structure. One end of the tube bundle array is completely sealed, while the other end is connected to an adapter. High-pressure hydrogen (100 MPa) is flushed into the adapter. When hydrogen is released, a tube bundle with an increased external length or diameter can be used to reduce the pressure to the desired range. A cross-sectional view of the

honeycomb structure is shown in Figure 1.

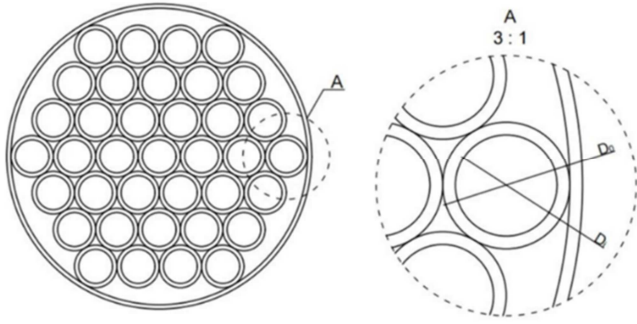


**Figure 1.** Cross-section of honeycomb structure.

In force analysis, cylinders are classified into thin-walled and thick-walled types according to the ratio of the outer

diameter to the inner diameter. Generally,  $K = D_o/D_i \leq 1.2$  defines a thin-walled cylinder, and  $K = D_o/D_i > 1.2$  defines a thick-walled cylinder, as shown in Figures 2 and 3, where  $D_i$  and  $D_o$  are the inner and outer diameters of the tube bundle, respectively. The structures proposed by Zhevago and collaborators for tube bundles use mostly thin-walled cylinders, and each cylinder has an outer hexagonal protective shell. The gap between the protective shell and cylinder is filled with plastic. Unlike those structures, the redundant hexagonal structure is omitted, and tube bundles with varying wall thicknesses are evaluated in this study. Based on membrane theory [10], stress can be expressed as

$$\begin{cases} \sigma_\theta = \frac{p_i D_i}{2\delta} \\ \sigma_z = \frac{p_i D_i}{4\delta} \end{cases} \quad (2)$$

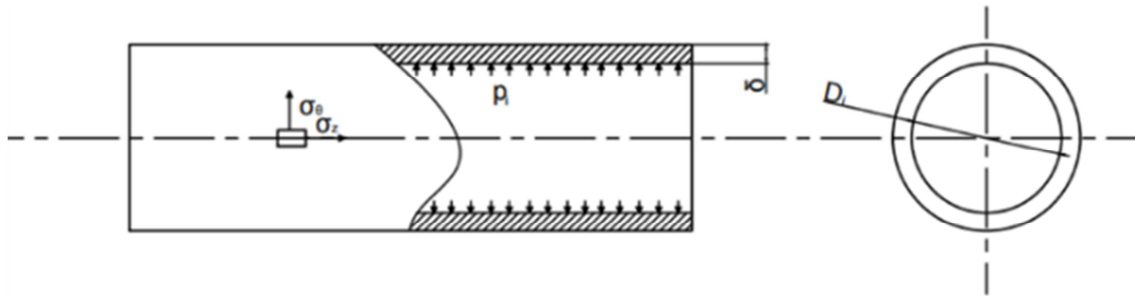


**Figure 2.** Thin-walled cylinder.

where  $\sigma_\theta$ ,  $\sigma_z$ , and  $p_i$  are the circumferential stress, longitudinal stress, and internal pressure of the tube bundle, respectively,  $\delta$  is the wall thickness. When the wall is very thin, the radial stress perpendicular to the container wall can be ignored. To reduce the calculation error, the inner diameter of the cylinder is changed into a middle diameter. Based on the Lamé function [11], the stress can be expressed as

$$\begin{cases} \sigma_\theta = \frac{p_i R_i^2 - p_o R_o^2}{R_o^2 - R_i^2} + \frac{(p_i - p_o) R_i^2 R_o^2}{R_o^2 - R_i^2} \frac{1}{r^2} \\ \sigma_r = \frac{p_i R_i^2 - p_o R_o^2}{R_o^2 - R_i^2} - \frac{(p_i - p_o) R_i^2 R_o^2}{R_o^2 - R_i^2} \frac{1}{r^2} \\ \sigma_z = \frac{p_i R_i^2 - p_o R_o^2}{R_o^2 - R_i^2} \end{cases} \quad (3)$$

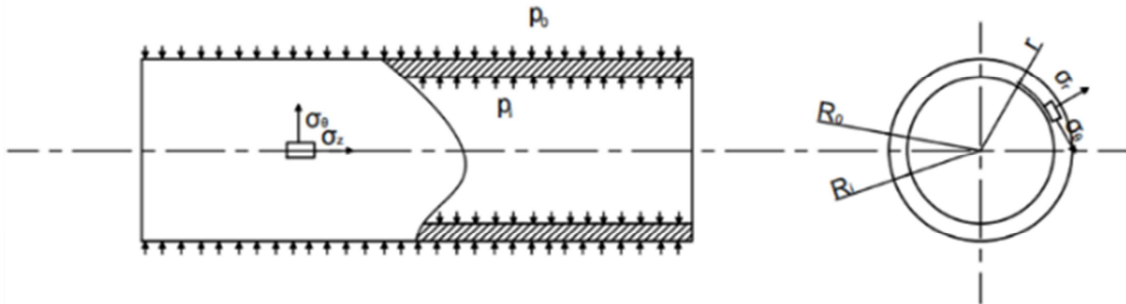


**Figure 3.** Thick-walled cylinder.

where  $\sigma_r$ ,  $p_o$ ,  $r$ ,  $R_i$ , and  $R_o$  are the radial stress, external pressure, finite element radius, inner radius, and outer radius of the tube bundle, respectively. Thus, the thickness of the cylinder cannot be ignored, and the circumferential and radial stresses change along the radial direction.

When a thick-walled cylinder is subjected to increasing

internal pressure, the inner surface is first plastic and expands outward, thus dividing the cylinder wall into plastic and elastic regions. The interface between the two regions is a cylindrical surface that is concentric with the cylinder [12]. Based on the micro-element equilibrium equation and von Mises yield criterion, the three-dimensional stress in the

plastic region can be expressed as

$$\begin{cases} \sigma_\theta = \frac{2}{\sqrt{3}} \sigma_s (1 + \ln \frac{r}{R_i}) - p_i \\ \sigma_r = \frac{2}{\sqrt{3}} \sigma_s \ln \frac{r}{R_i} - p_i \\ \sigma_z = \frac{\sigma_s}{\sqrt{3}} (1 + 2 \ln \frac{r}{R_i}) - p_i \end{cases} \quad (4)$$

Because the plastic and elastic regions belong to a continuum, the stress in the elastic region is given by

$$\begin{cases} \sigma_\theta = \frac{\sigma_s R_C^2}{\sqrt{3} R_0^2} (1 + \frac{R_0^2}{r^2}) \\ \sigma_r = \frac{\sigma_s R_C^2}{\sqrt{3} R_0^2} (1 - \frac{R_0^2}{r^2}) \\ \sigma_z = \frac{\sigma_s R_C^2}{\sqrt{3} R_0^2} \end{cases} \quad (5)$$

where  $R_c$  is the radius of the interface and  $p_c$  is the pressure on the interface. The first strength theory is used to determine whether the glass tube bundle is broken:

$$\sigma_1 \leq [\sigma] \quad (6)$$

where  $\sigma_1$  is the maximum stress. To accurately calculate the PVT relationship of hydrogen in simulations, the Redlich–Kwong real gas equation of state can be applied [13]. In terms of the DOE standard [14], weight capacity  $G_C$  and volume capacity  $V_C$  of hydrogen in a glass tube bundle can be expressed as

$$G_C = \frac{\rho S}{\rho S + w} \quad (7)$$

$$V_C = \frac{\rho D_i^2}{D_0^2} \quad (8)$$

where  $\rho$ ,  $s$ , and  $w$  are the hydrogen density, cross-sectional area of the inner cavity, and weight per unit length of the tube bundle, respectively.

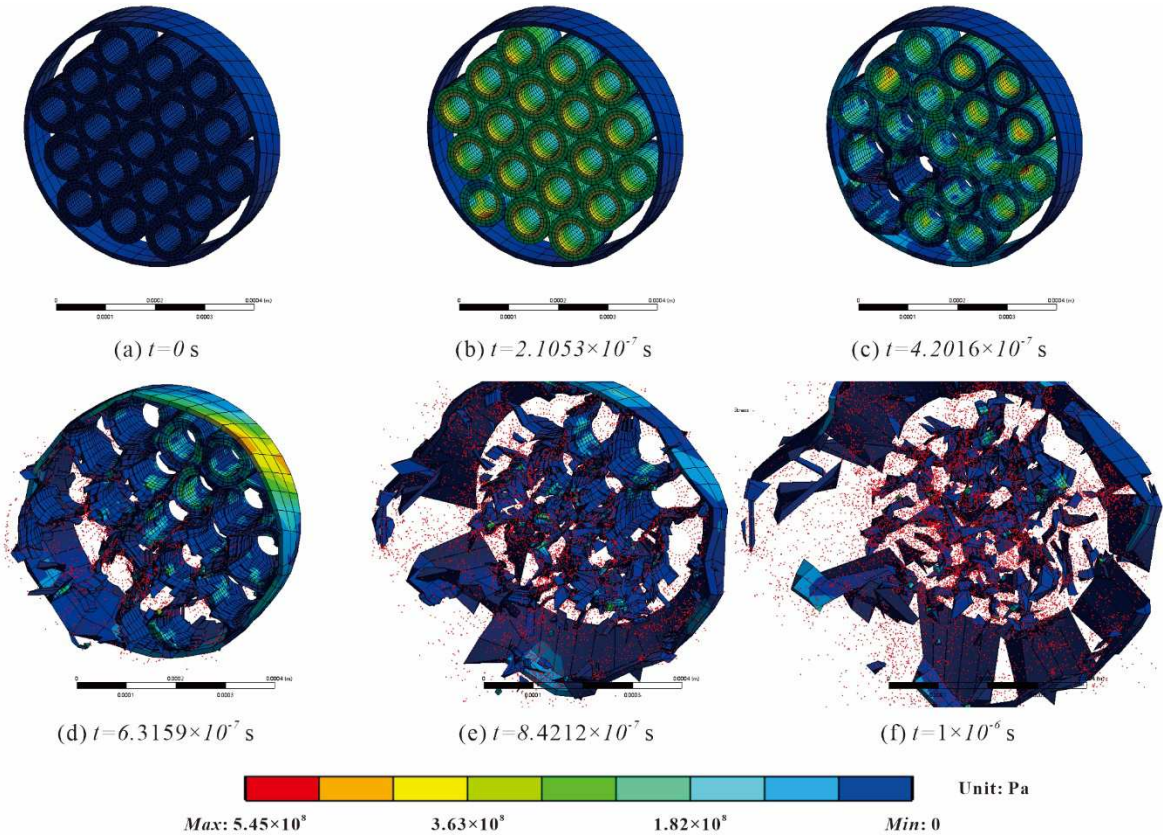


Figure 4. Crushing simulation of 19 tubes in a bundle.

### 3. Simulation of Glass Tube Bundle

The Ansys Workbench was used to perform finite element calculations. Because one end of the tube bundle is fixed, the stress follows a gradient distribution along the tube bundle. However, compared with the stress caused by internal high-pressure hydrogen, it can be ignored [15]. To simplify calculations, the length of the tube bundle can be shortened,

without notably affecting the final results. The results from a crushing simulation of 19 tubes in a bundle are illustrated in Figure 4.

#### 3.1. Evaluation of Number of Tubes in a Bundle

By adding tubes, each tube bundle expands by internal pressure, causing extrusion between the tubes. The ultimate stress ( $\sigma_1$ ) and volume expansion rate of the various tube bundles ( $p$ ) are shown in Figure 5. Stress  $\sigma_1$  of a single tube



bundle with an inner diameter of 30  $\mu\text{m}$  and outer diameter of 50  $\mu\text{m}$  is 130 MPa. The number of tube bundles has a negligible effect on  $\sigma_1$  and  $p$ . Nevertheless, the difference between a single tube and multiple tubes is considerable. Compared with a single tube,  $\sigma_1$  and  $p$  of multiple tubes are greatly reduced, but the differences between multiple tubes are small. With an increasing number of tube bundles, the two parameters tend to stabilize.

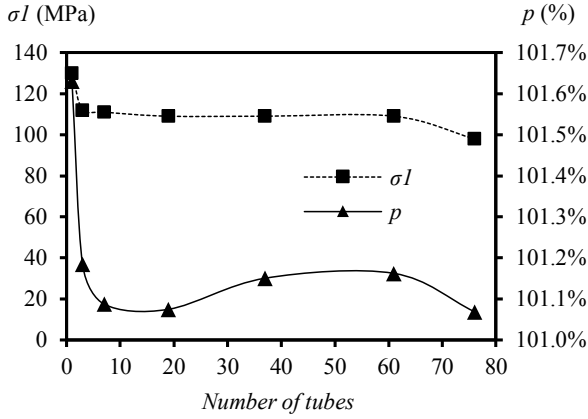


**Figure 5.** Effect of number of tubes on stress  $\sigma_1$  and volume expansion  $p$ .

Volume capacity  $V_C$  and weight capacity  $G_C$  according to the number of tubes are compared in Figure 6. Again, a notable difference exists between a single tube and multiple tubes, with the latter showing a stable trend regardless of increasing the number of tubes.

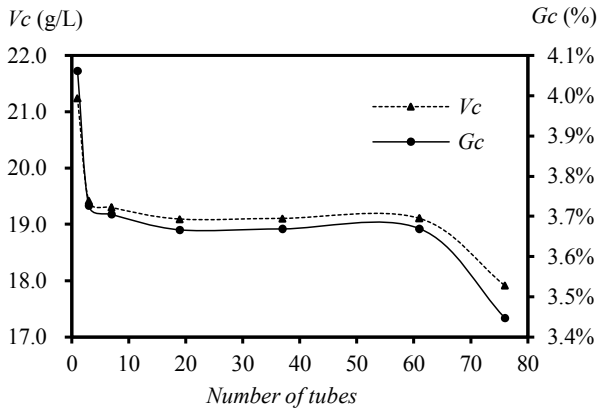


**Figure 6.** Effect of number of tubes on weight capacity  $G_C$  and volume capacity  $V_C$ .

### 3.2. Evaluation of Coating Material

Regarding bundle crushing (Figure 4), the tubes on the bundle periphery are important, and the robustness may be related to the material of the protective sleeve. A protective sleeve made of glass fiber, low-carbon steel, or rubber is used for evaluation. Compared with the glass of the tubes, the toughness of the sleeve is the same, higher, and lower, respectively. The impact of the three sleeve materials on  $\sigma_1$ ,  $p$ ,  $V_C$ , and  $G_C$  of the bundle according to the number of tubes is shown in Figures 7 and 8.

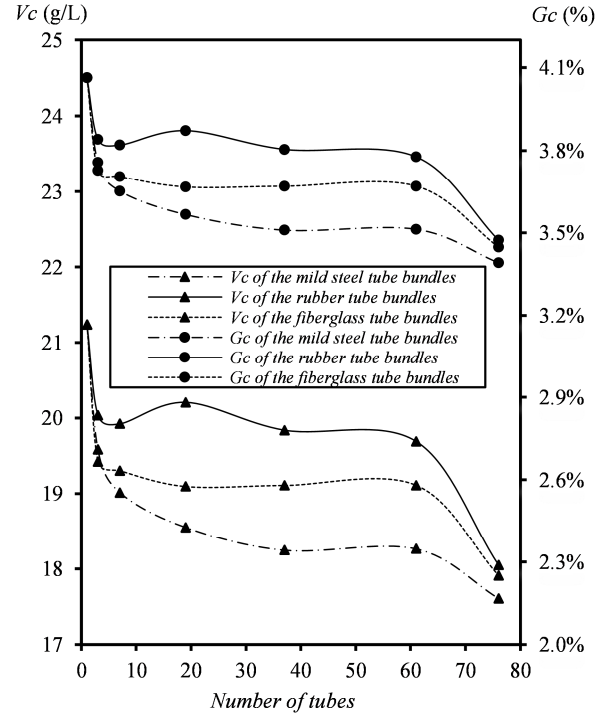


**Figure 7.** Effect of protective sleeve material on stress  $\sigma_1$  and volume expansion  $p$ .

The number of tube bundles among multiple tubes has a small effect on its performance. Meanwhile, the material of the protective sleeve affects performance. Compared with the protective sleeve made of low-carbon steel, the protective sleeve made of rubber has better  $\sigma_1$ ,  $p$ ,  $V_C$ , and  $G_C$ , indicating that a tougher protective sleeve increases performance.

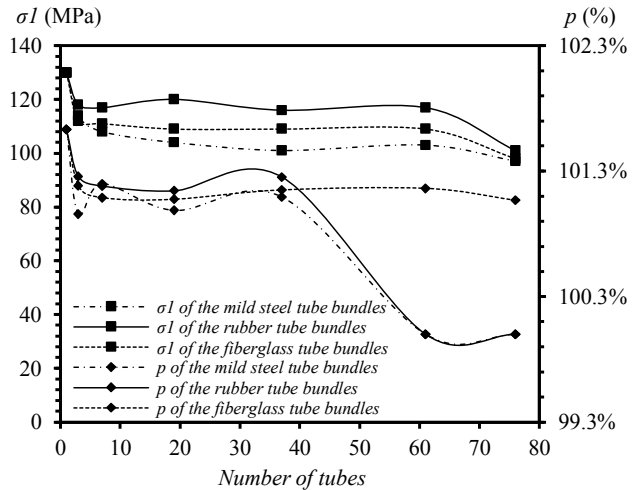


**Figure 8.** Effect of protective sleeve material on weight capacity  $G_C$  and volume capacity  $V_C$ .

### 3.3. Evaluation of Tube Wall Thickness

Based on the membrane theory and Lamé formula, the wall thickness of the tube bundle has considerable effects on  $\sigma_1$ ,  $V_C$ , and  $G_C$ . Therefore, different wall thicknesses are evaluated for an inner diameter of 30  $\mu\text{m}$ . The corresponding changes in  $\sigma_1$ ,  $p$ ,  $V_C$ , and  $G_C$  are shown in Figures 9 and 10.

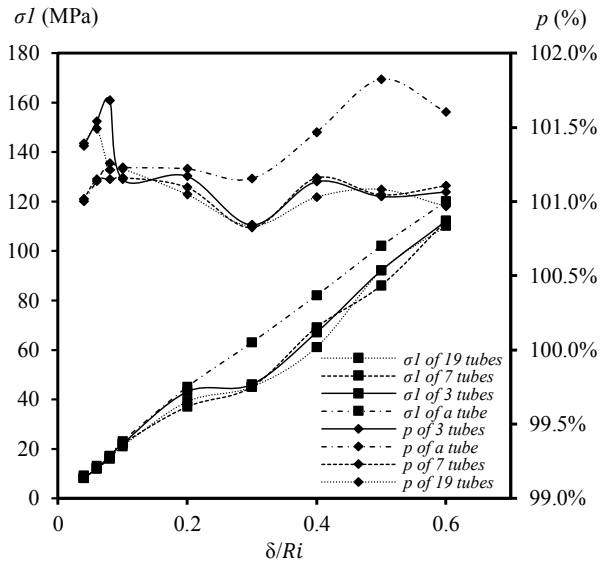


Figure 9. Effect of wall thickness  $\delta/R_i$  on stress  $\sigma_1$  and volume expansion  $p$ .

Stress  $\sigma_1$  increases almost linearly with increasing wall thickness. Volume expansion  $p$  of a single tube increases slightly, whereas that of multiple tubes remains basically unchanged. In addition, with increasing wall thickness, weight capacity  $G_C$  decreases, and volume capacity  $V_C$  increases.

Overall, the experimental results obtained by Zhevago et al. [2] are consistent with the trends observed in the simulation results of this study. Although the results slightly differ from the DOE standard, the trends are correct. The main reason for this difference is that the strength of the selected glass fiber material is lower than expected. Moreover, the data obtained before calculation has a low value in experiments, and the actual strength is higher than the calculated strength.

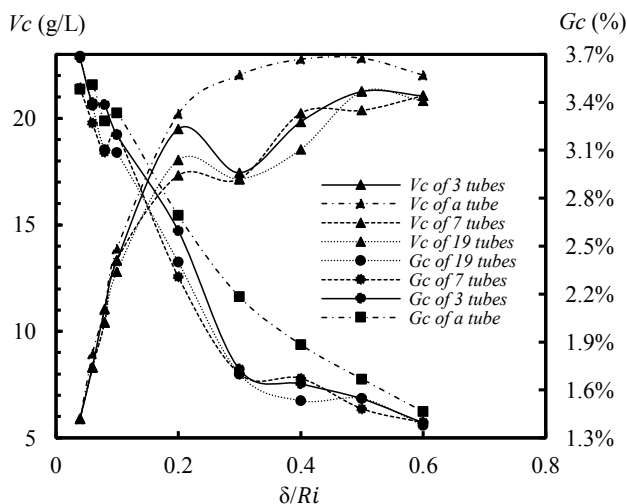


Figure 10. Effect of wall thickness  $\delta/R_i$  on weight capacity  $G_C$  and volume capacity  $V_C$ .

## 4. Conclusion

Based on the results of this study, the following conclusions can be drawn:

- 1) The number of tubes has a small effect on the tube bundles, and the main effect difference is observed between a single tube and multiple tubes. Compared with a single tube, stress  $\sigma_1$ , volume expansion  $p$ , volume capacity  $V_C$ , and weight capacity  $G_C$  decrease with multiple tubes. However, the differences between multiple tubes are small.
- 2) The material of the tube bundle protective sleeve affects the characteristics of the tube bundle. A tougher sleeve material results in higher values for the tube bundle parameters.
- 3) The wall thickness of the tubes has the greatest effect on the bundle. With increasing wall thickness,  $\sigma_1$  and  $V_C$  increase, while  $G_C$  decreases. On the other hand,  $p$  remains stable.

One limitation of the study is that the obtained results slightly differ from the DOE standard. The main reason for this is that the strength of the selected glass fiber material is lower than expected. In the future, studies may be conducted to improve the strength of the material and the machining accuracy.

## Acknowledgements

This research was supported by Shenzhen Science and Technology Innovation Commission (No. KCXFZ20201221173608021).

## References

- [1] Zheng. J, Ou. K, Hua. Z, Xu. P, He. Y, Zhao. Y, Han. B. (2014). Research on local fire test method of high-pressure hydrogen storage cylinder for vehicles. *Journal of Solar Energy*, 35 (01), 58-63.
- [2] N. K. Zhevago. (2010). Experimental investigation of hydrogen storage in capillary arrays. *International Journal of Hydrogen Energy*, 35 (1), 169-175. doi: 10.1016/j.ijhydene.2009.10.011.
- [3] Li. X, Bi. J, Ke. D. (2013). Thermodynamic model of leakage in a high-pressure hydrogen storage system. *Journal of Tsinghua University (Natural Science Edition)*, 53 (04), 503-508. doi: 10.16511/j.cnki.qhdxxb.2013.04.027.
- [4] Yan. X. (2022). Research on hydrogen storage technology methods. *Energy & Energy Conservation*, (05), 59-61. doi: 10.16643/j.cnki.14-1360/td.2022.05.037.
- [5] Anna Grzech, Jie Yang, Piotr J. Glazer, Theo J. Dingemans, Fokko M. Mulder. (2014). Effect of long range van der Waals interactions on hydrogen storage capacity and heat of adsorption in large pore silicas. *International Journal of Hydrogen Energy*, 39 (9), 4367-4372. doi: 10.1016/j.ijhydene.2013.12.134.
- [6] N. K. Zhevago, V. I. Glebov. (2007). Hydrogen storage in capillary arrays. *Energy Conversion and Management*, 48 (5), 1554-1559. doi: 10.1016/j.enconman.2006.11.017.
- [7] R. Gerboni. (2016). Introduction to hydrogen transportation. *Compendium of Hydrogen Energy*, 2 (11), 283-299. doi: 10.1016/B978-1-78242-362-1.00011-0.

- [8] Niu. Z, Cao. L, Li. Q. (2021). Application and research status of glass fiber reinforced composites. *Plastics Industry*, 49 (S1), 9-17.
- [9] Wen. F. (2021). Study on mechanical properties of carbon glass fiber mixed ribs. Zhengzhou University. doi: 10.27466/d.cnki.gzzdu.2021.002738.
- [10] Liu. Y, Wu. J, Sun. J. (2014). Theoretical calculation of blasting pressure of airbags for ship launching. *Rubber industry*, 61 (09), 554-556.
- [11] Li. Z, Li. Y, Tang. A. (2020). Analysis of plastic deformation conditions and brittleness of thick-walled cylinders under internal pressure. *Chinese Journal of Applied Mechanics*, 37 (04), 1515-1520+1857.
- [12] Lu. Z (2009). Reliability Design of Pressure Vessel Shell and Its Application in Solid Rocket Motor Shell. Beijing Jiaotong University.
- [13] Liu, G, Qin. Y, Liu. Y. (2021). Numerical simulation of hydrogen filling process in novel high-pressure microtube storage device. *International Journal of Hydrogen Energy*, 46 (74), 36859-36871. doi: 10.1016/j.ijhydene.2021.08.227.
- [14] N. K. Zhevago, E. I. Denisov, V. I. Glebov, S. V. Korobtsev, A. F. Chabak (2013). Storage of cryo-compressed hydrogen in flexible glass capillaries. *International Journal of Hydrogen Energy*, 38 (16), 6694-6703. doi: 10.1016/j.ijhydene.2013.03.107.
- [15] Yao. C. (2021). Stress assessment and fatigue analysis of hydrogen storage tank inflation process of hydrogen energy fuel cell ship. Harbin Institute of Technology. doi: 10.27061/d.cnki.ghgdu.2021.004825.